

are given in Tables XVI and XVII. As can be seen in Table XVIII, the calculated heats of formation are in excellent agreement with the experimental values, with one exception, diisopropylamine. This number is so far off we concluded the experimental value must be in error, and we did not weight this compound in the parameterization. (Ab initio calculations recently confirmed that the experimental value is indeed in error.⁴⁹)

(49) Allinger, N. L.; Schmitz, L. R.; Motoc, I.; Bender, C.; Labanowski, J. K. *J. Phys. Org. Chem.* In press.

(50) Experimental heats of formation are taken from the following: (a) Cox, J. D.; Pilcher, G. *Thermochemistry of Organic and Organometallic Compounds*; Academic Press: London, 1970. (b) Pedley, J. B.; Naylor, R. D.; Kirby, S. P. *Thermochemical Data of Organic Compounds*; Chapman and Hall: London, 1977.

Strain energies may be calculated in the usual way.¹ (Further discussion is given in the MM2(87) (and earlier) and MM3 manuals.) The strainless group increments were fit for the group of compounds as shown by the input in Table XIX. The strainless increment for the 8-56 bond was arbitrarily set equal to that of a C-N (1-8) bond, and the strainless increment for NCBU was set to zero. The results are given in Table XX.

The complete set of structural parameters (which must be added to those already developed for alkanes⁶) for amines is given in Table XXI.

Acknowledgment. The authors are indebted to the National Science Foundation (Grant No. CHE 8614548) and to the National Institutes of Health (Grant No. R24RR02165) for partial support of this work.

NMR Study of Heme Pocket Polarity/Hydrophobicity of Myoglobin Using Polypropionate-Substituted Hemins

Jón B. Hauksson, Gerd N. La Mar,* Ravindra K. Pandey, Irene N. Rezzano, and Kevin M. Smith

Contribution from the Department of Chemistry, University of California, Davis, California 95616. Received April 2, 1990

Abstract: The products of the reconstitution of sperm whale apomyoglobins with a series of synthetic hemins possessing a wide variety of substitution patterns for two and three propionates on the methyl-containing heme periphery were studied by NMR in the metaquo and metcyano derivatives to investigate the prospects for, and structural and thermodynamic consequences of, the location of propionates in the hydrophobic interior of the pocket. The orientations for the propionates for the various hemins were determined by the nuclear Overhauser effect in the metcyano complexes. In all but one case, a single, unique orientation was found for each hemin which resulted in the occupation by a propionate, in at least one case, in each of the possible eight heme pocket sites without disruption of the heme pocket structure. While propionate orientations into the protein interior were readily attainable, indicating a surprising polar pocket environment, these propionates exhibited extraordinarily elevated $pK_s > 8$ indicative of the highly hydrophobic contacts in the interior of the heme pocket. For propionates situated in the sites of the usual protohemin vinyl groups, we observe pH-modulated structural transitions involving deprotonation of the propionate that results in changes in the orientations of the hemins. The detection of saturation transfer between these alternate orientations identifies the interconversion mechanism as rotational "hopping" of the hemin about the intact iron-histidine bond. The thermodynamics of the carboxylate side chains and dynamics of isomer interconversion can serve as sensitive probes of heme pocket structure among both natural and synthetic myoglobin variants.

Introduction

The heme pockets of the molecular oxygen binding hemoproteins, myoglobin, Mb, and hemoglobin, Hb, are generally described as hydrophobic and nonpolar except for a region near the protein surface where the ubiquitous hydrophilic heme propionate side chains make salt bridges to the protein matrix.¹⁻⁴ The apparently apolar environment of most of the heme pocket is supported by the large number of heme-protein contacts with nonfunctionalized aliphatic and aromatic side chains, particularly in the region of the vinyl bearing pyrroles of the native protohemin prosthetic group. Recent spectroscopic investigations of complexes of sperm whale apomyoglobin, apoMb, with a dye intercalated into the heme pocket,⁵ however, have suggested that the heme pocket of Mb may be more polar than previously thought.⁴ The overwhelming preference for the ubiquitous 6,7-propionate groups for the unique orientations as described in numerous X-ray

crystallographic^{2,3} studies provides another measure of the relatively localized hydrophobic and hydrophilic regions of the heme pocket. While it is now recognized that the heme can sit in the pocket in more than one orientation, at least initially during assembly of holoprotein from hemin and apoMb,^{6,7} and at equilibrium for some Mbs and Hbs,⁸⁻¹¹ this transient or equilibrium orientational disorder leaves the two salt bridges unaltered and simply permutes the hydrophobic contacts. This hydrophobic region of the heme pocket of Mb is found to be remarkably adaptable in that hemins with bulky substituents readily incorporate into an otherwise essentially unperturbed holoprotein.¹² Recent studies with hemins possessing a single propionate group¹³

(6) La Mar, G. N.; Budd, D. L.; Viscio, D. B.; Smith, K. M.; Langry, K. C. *Proc. Natl. Acad. Sci. U.S.A.* **1978**, *75*, 5755-5759.

(7) La Mar, G. N.; Toi, H.; Krishnamoorthi, R. *J. Am. Chem. Soc.* **1984**, *106*, 6395-6400.

(8) Levy, M. J.; La Mar, G. N.; Jue, T.; Smith, K. M.; Pande, R. K.; Smith, W. S.; Livingston, D. J.; Brown, W. D. *J. Biol. Chem.* **1985**, *260*, 13694-13698.

(9) Peyton, D. H.; La Mar, G. N.; Pande, U.; Ascoli, F.; Smith, K. M.; Pandey, R. K.; Parish, D. W.; Bolognesi, M.; Brunori, M. *Biochemistry* **1989**, *28*, 4880-4887.

(10) Cooke, R. M.; Wright, P. E. *Eur. J. Biochem.* **1987**, *166*, 409-414.

(11) Peyton, D. H.; La Mar, G. N.; Gersonde, K. *Biochim. Biophys. Acta* **1988**, *954*, 82-94.

(12) Miki, K.; Ii, Y.; Yokawa, M.; Owatari, A.; Hato, Y.; Harada, S.; Kai, Y.; Kasai, N.; Hata, Y.; Tanaka, N.; Karuda, M.; Katsubi, Y.; Yoshida, Z.; Ogoshi, H. *J. Biochem.* **1986**, *100*, 269-270.

(1) Antonini, E.; Brunori, M. *Hemoglobin and Myoglobin in Their Reactions with Ligands*; North Holland Publishing Company: Amsterdam, **1971**; pp 55-97.

(2) (a) Takano, T. *J. Mol. Biol.* **1977**, *110*, 537-568. (b) Phillips, S. E. V. *J. Mol. Biol.* **1980**, *192*, 133-154. (c) Kuriyan, J.; Wilz, S.; Karplus, M.; Petsko, G. A. *J. Mol. Biol.* **1986**, *192*, 133-154.

(3) (a) Fermi, G. *J. Mol. Biol.* **1975**, *97*, 237-256. (b) Baldwin, J. J. *J. Mol. Biol.* **1980**, *136*, 103-128.

(4) Stryer, L. *J. Mol. Biol.* **1965**, *13*, 482-495.

(5) Macgregor, R. B.; Weber, G. *Nature* **1986**, *319*, 70-73.

and protohemin-type isomers possessing permuted methyl/propionate substituents¹⁴ have provided evidence that there is little intrinsic difference in the preference for formation of the two native propionate salt bridges and that propionates can be accommodated in the heme pocket at positions other than those found in the native protein, with at least one of them being in the hydrophobic pocket interior.

In this report we expand our investigation of the intrinsic hydrophobicity of the heme pocket of sperm whale Mb by structurally characterizing the holoproteins reconstituted with a series of synthetic hemins designed to force, if possible, the occupation of a propionate group at each of the eight potential sites described by the heme skeleton in the native structure. These sites, identified as a–h in 1 of Figure 1, are normally occupied by protohemin substituent 1–8 in the single crystal hemin orientation.²³ Questions we seek to answer are the following: (1) Is there a unique orientation of the heme? (2) What are the limitations as to where propionates can be sited in a completely folded holoprotein? (3) What are the relative preferences for the occupation of the relative sites? (4) To what extent is the ground-state molecular/electronic structure of the heme cavity perturbed by the occupation by propionates of non-native sites? (5) How are the pKs of the propionate influenced by non-native sites? (6) Does the seating of propionates (or heme orientation) depend on the state of propionate protonation?

The chemical modification of the hemin by total synthesis¹⁵ to introduce potentially charged groups in non-native regions of the heme is, in many respects, an attractive alternative and with the obvious parallels to current studies on site-directed mutagenesis of the polypeptide chain.¹⁶ The selected hemins containing all isomers possessing two propionates and six methyls are identified as 2, 6–10 in Figure 1; only 2 possesses the two propionates positioned on the hemin such that they can form the unperturbed propionate links of the native protein.^{1–3} Three hemins with these "native" pairs of propionates found in 2, but with each possessing an additional "odd" propionate at the three possible isomeric positions, are described in structures 3–5 in Figure 1. These latter three hemins were designed not only to guarantee population of non-native sites but also to provide direct information on the pairwise occupational preference about the conventional α,γ -meso axis of native protohemin.^{7,8}

The positions occupied by propionates will be determined by establishing the absolute orientation of the hemin with the protein matrix. This is achieved in solution most readily by using ¹H NMR of the paramagnetic metMbCN derivative, as demonstrated^{17–19} in great detail for the native protein^{17–20} as well as apoMb reconstituted with 2.²¹ The technique is to identify, pairwise, first the resonances of neighboring heme substituents and then the resonances of select heme pocket residues in close contact with the heme and lastly to establish a unique stereochemistry for the heme substituents relative to the heme pocket residues, each step relying on the nuclear Overhauser effect NOE.^{17–22} An auxiliary method for establishing the orientation is based on the contact shift pattern exhibited by the assigned hemin substituents. This pattern is determined completely by the orientation of the axial His F8 imidazole plane^{23,24} and can be

taken as essentially invariant in the holoproteins. The ranges of contact shifts exhibited by heme methyls at all eight positions in the protein matrix, a–h, have been established²¹ and are presented schematically in A of Figure 2. Information on the nature of perturbation on the electronic/molecular structure of intact proteins can be assessed by the hyperfine shifts which characterize the low-spin, metcyano^{17–24} and high-spin, metaquo^{24,25} Mb complexes.

Experimental Section

Reconstitution of Myoglobin. Sperm whale myoglobin was purchased from Sigma Chemical Company and used without further purification. Apomyoglobin, apoMb, was prepared according to published procedures.²⁶ For metcyano Mb samples, solutions approximately 1.5 mM in apoMb in ²H₂O were prepared by dissolving lyophilized apoMb in cold phosphate buffer (50 mM, pH 6.2–6.3). The precipitate, if any, was removed by centrifugation, and the final concentration of apoprotein was determined by optical absorption intensity ($\epsilon = 15900 \text{ M}^{-1} \text{ cm}^{-1}$ at 280 nm). For metaquo samples, solutions approximately 1.5 mM in apoMb in ²H₂O were prepared by dissolving lyophilized apoMb in cold NaCl solution (0.1 M, pH 6.2–6.3).

The hemins were prepared, and iron was inserted as reported previously.^{15,27} For metaquo myoglobin samples, 10 molar equiv of hemin were prepared by dissolving them in 0.2 M NaO²H; for metcyano Mb samples, a 5–6-fold excess potassium cyanide was added. Each reconstituted protein was prepared by dropwise addition of 1 molar equiv of the hemin solution to the chilled apoMb solution. The reaction of apoMb with hemin was monitored optically to verify 1:1 incorporation of hemin into the apoprotein by using the characteristic shift of the Soret peak.²⁸ The metmyoglobins have an absorbance ratio A_{Soret}/A_{280} of ≥ 3 , with a Soret maximum of 395 nm for the metaquo and 408 nm for the metcyano Mb complexes. Visible absorption peaks are observed at 496 and 626 nm for the metaquo and at 534 nm for the metcyano Mb complexes. The optical spectra of the complex of hemins 3–10 were essentially superimposable on that of the previously characterized complexes of heme 2.²¹ The pH of each metaquo sample was adjusted to a value between 6.2 and 6.5, and any precipitate was removed by centrifugation and then transferred to a 5-mm NMR tube for immediate NMR measurement. The metcyano myoglobin samples were concentrated to ~ 2 mM in an Amicon ultrafiltration cell, and the solvent was exchanged several times with ²H₂O, 0.2 M in NaCl, and 0.020 M in KCN. The sample pH was measured with a Beckman 3550 pH meter equipped with an Ingold microcombination electrode; pH values were not corrected for the isotope effect.

¹H NMR Measurements. ¹H-NMR spectra were recorded on Nicolet NT-360 and NM-500 FT NMR spectrometers by using quadrature phase detection at 360 and 500 MHz, respectively. For the metaquo Mb (metMbH₂O) samples, spectra were recorded by collecting 8192 data points over a 45-kHz bandwidth at a pulse repetition rate of 10 s^{-1} at 360 MHz, typically requiring 4000–6000 transients. For metcyano Mb (metMbCN) samples, spectra were collected in double precision by using 16384 data points over a 14-kHz bandwidth at a pulse repetition rate of 1 s^{-1} at 500 MHz. In both cases the residual water signal was suppressed with a low-power decoupler pulse.

The pH titrations of the metMbCN complexes reconstituted with hemins 4, 5, 6, 9, and 10 were performed over the range ~ 5 to ~ 10 , by adding 0.2 M NaO²H in ²H₂O dropwise to an acidified solution. The spectra of the complexes of the other hemins were recorded at pH 8.0 and 10.0. All pH effects are shown to be reversible by back-titration of the pH in small increments. The samples spent 20–25 min at each pH value before initiation of NMR measurements.

Most of the synthetic hemins, 3–10, were available only in limited supply and afforded protein samples sufficiently concentrated for 1D steady-state nuclear Overhauser effect, NOE, studies^{21,22} but were too low for practical 2D NOESY experiments.²⁰ Steady-state NOE difference spectra were recorded by applying a presaturation pulse of 200 ms duration with the decoupler on-resonance and subtracting it from a corresponding reference spectrum recorded under identical conditions but with the decoupler off-resonance. On- and off-resonance frequencies

(13) Hauksson, J. B.; La Mar, G. N.; Pandey, R. K.; Rezzano, I. K.; Smith, K. M. *J. Am. Chem. Soc.* In press.

(14) Hauksson, J. B.; La Mar, G. N.; Pande, U.; Pandey, R. K.; Parish, D. W.; Singh, J. P.; Smith, K. M. *Biochim. Biophys. Acta* In press.

(15) Pandey, R. K.; Rezzano, I. N.; Smith, K. M. *J. Chem. Res.* **1987**, 2172–2192.

(16) Varadarajan, R.; Lambright, D. G.; Boxer, S. G. *Biochemistry* **1989**, 28, 3771–3781.

(17) Ramaprasad, S.; Johnson, R. D.; La Mar, G. N. *J. Am. Chem. Soc.* **1984**, 101, 5330–5335.

(18) Emerson, S. D.; Lecomte, J. T. J.; La Mar, G. N. *J. Am. Chem. Soc.* **1988**, 110, 4176–4182.

(19) Lecomte, J. T. J.; Johnson, R. D.; La Mar, G. N. *Biochim. Biophys. Acta* **1985**, 829, 268–274.

(20) Emerson, S. D.; La Mar, G. N. *Biochemistry* **1990**, 29, 1545–1555.

(21) La Mar, G. N.; Emerson, S. D.; Lecomte, J. T. J.; Pande, U.; Smith, K. M.; Craig, G. W.; Kehres, L. A. *J. Am. Chem. Soc.* **1986**, 108, 5568–5573.

(22) Neuhaus, D.; Williamson, M. *The Nuclear Overhauser Effect*; VCH Publishers: New York, 1989; Chapter 2.

(23) Shulman, R. G.; Glarum, S. H.; Karplus, M. *J. Mol. Biol.* **1971**, 57, 93–115.

(24) La Mar, G. N. In *Biological Applications of Magnetic Resonance*; Shulman, R. G., Ed.; Academic Press: New York, 1979; pp 305–340.

(25) La Mar, G. N.; Budd, D. L.; Smith, K. M.; Langry, K. C. *J. Am. Chem. Soc.* **1980**, 102, 1822–1827.

(26) Teale, F. W. J. *Biochim. Biophys. Acta* **1959**, 35, 563.

(27) Smith, K. M.; Fujinari, E. M.; Langry, K. C.; Parish, D. W.; Tabba, H. D. *J. Am. Chem. Soc.* **1983**, 105, 6638–6646.

(28) Asakura, T.; Yonetani, T. *J. Biol. Chem.* **1969**, 244, 4573–4579.

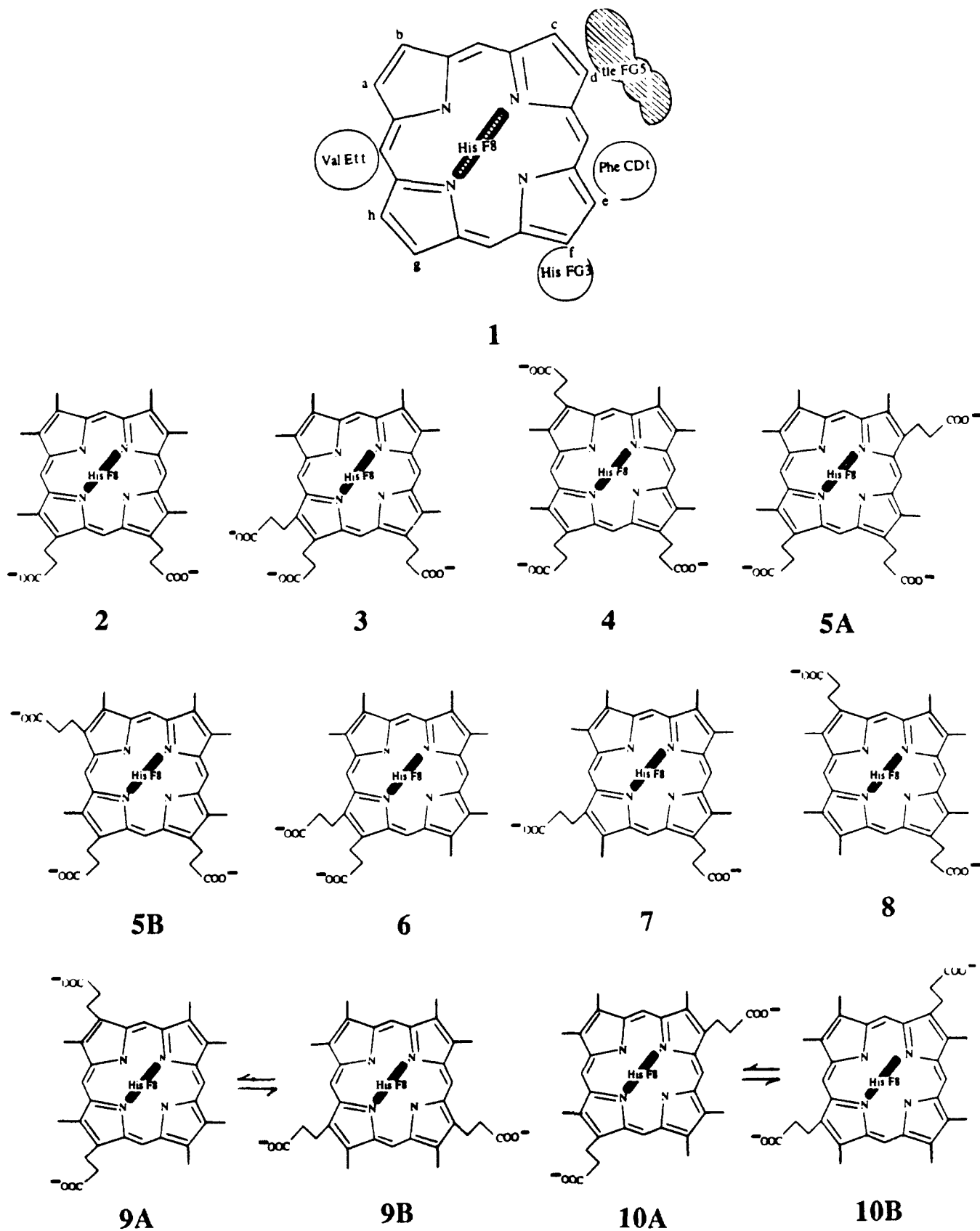


Figure 1. Schematic structure of the heme skeleton, 1, as oriented in the heme pocket of Mb, with the key adjacent amino acid residues, Ile FG5, Phe CD1, His FG3, Val E11, and His F8. The various pyrrole positions are indicated by a protein-based labeling scheme, a-h, that identifies substituents on the heme by their location in the protein matrix, rather than on the heme. For native protohemin, the positions a-h are occupied by substituents numbered 1-8. The correlation of the known heme structure and the determined protein seating of assigned substituents leads to the orientation of the heme in the pocket. The chemical structures of a variety of modified hemins possessing solely methyls and propionate substituents on the pyrroles and the orientation determined by NOE measurements are given in 2-10. The hemins with more than one orientation are appended by A and B, i.e., 5A and 5B. The heme pocket is viewed from the same vantage point in 1 and 2-10, except that only the rectangle reflecting the His F8 imidazole side chains orientation is included in the latter.

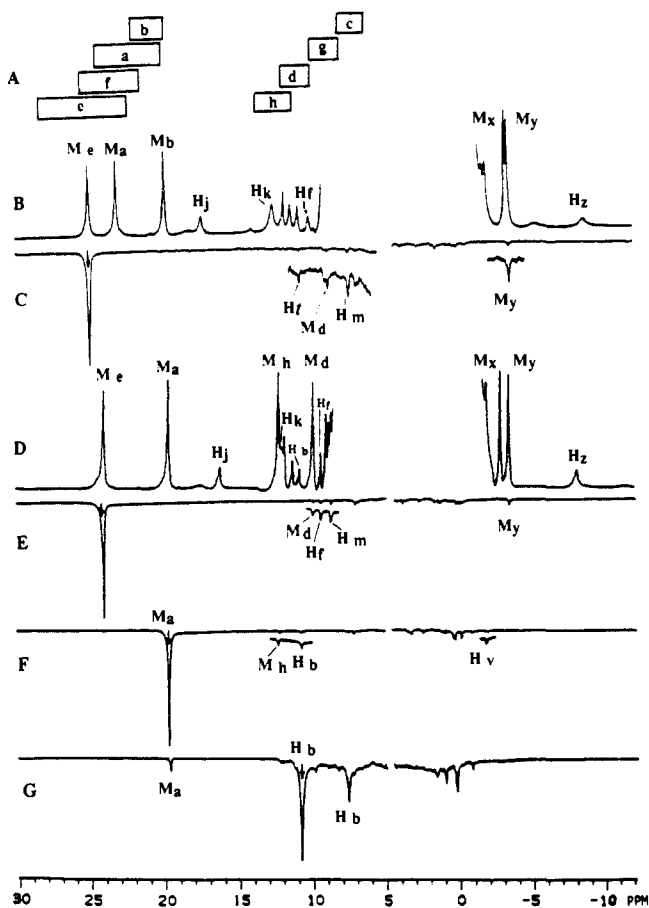


Figure 2. (A) Schematic representation of the known range of chemical shifts exhibited by a methyl group as characterized solely by its position in the alternate sites of the protein-based labeling scheme, a–h, as depicted in 1 of Figure 1; note that only five methyls (a, b, e, f and h) are predicted to exhibit shifts downfield of 12 ppm. (B) 500-MHz ^1H -NMR reference trace of the metMbcCN complex of hemin 3 in $^2\text{H}_2\text{O}$, pH 8.6 at 25 $^\circ\text{C}$, with peaks labeled M_i , H_i for methyls and single protons. (C) Saturate M_e ; note NOEs to H_m (Phe CD1 $\text{C}_\delta\text{H}_s$), M_y (Ile FG5 C_βH_3), M_d , and H_f . (D) 500-MHz ^1H -NMR reference trace for hemin 4 reconstituted into metMbcCN, in $^2\text{H}_2\text{O}$ at pH 8.55 and 30 $^\circ\text{C}$. (E) Saturate M_e ; note NOEs to Phe CD1 $\text{C}_\delta\text{H}_s$ (H_m) and Ile FG5 (M_y) as well as M_d and H_f . (F) Saturate M_a ; note NOE to M_h and H_b . (G) Saturate H_b ; note reciprocal NOE to M_a and very large NOE to H_b' , which identifies a propionate $\alpha\text{-CH}_2$ in protein site b in 1 of Figure 1.

were alternated every 100 scans. Typical spectra consisted of at least 2600 transients with a repetition rate of 1 s^{-1} . Chemical shifts for all the spectra are referenced to DSS (2,2-dimethyl-2-silapentane-5-sulfonate) through the residual water resonance.

Results

Reconstitution Heterogeneity. The stoichiometric 1:1 incorporation of each of the eight modified hemins 3–10 into a heme pocket largely unperturbed from that of the native protein is confirmed both by the clean breaks in the optical titrations²⁸ and by the optical bands for both metaquo and metcyano complexes which are found essentially indistinguishable for those of the hemin derivative 2 which has its propionate at the same sites as for native protohemin. Moreover, optical pH titrations fail to reveal any significant spectral perturbations for the metMbcCN complex over the pH range 5.5–10 (not shown), indicating the retention of the holoprotein structure over a broad pH range.

^1H NMR spectra recorded as soon after reconstitution as possible (20–30 min) were the same as after considerable equilibration times (several months), both for the metMbH₂O (see supplementary material) and metMbcCN derivatives. Moreover, except for hemin 5, the ^1H NMR spectra for the metMbcCN complexes at acidic to neutral pH are consistent at all times with a single and unique species with a series of resonances of relative intensities 3 and 1, reflecting methyl and single proton peaks. Only

for the complexes of hemin 5 could we find evidence for a second equilibrium molecular species at neutral pH which could not be traced to an impurity in the hemin (see below). Hence we consider further structural characterization on protein complexes assumed to be at equilibrium.

NOE-Determined Heme Orientation at Neutral pH. The resonances in the ^1H NMR spectra of the metMbcCN complex are labeled M_i , H_i for methyls and single protons, respectively, of the dominant isomer; m_i , h_i have similar significance for any equilibrium minor isomer. The subscripts i refer to the position of the heme substituent in the protein-based site labeling, a–h, as shown in 1 of Figure 1. The subscripts j, k, m and w, x, y, z identify resonances for Phe CD1 and Ile FG 5, respectively,^{17,18} with subscripts n and v describing important His FG3 C_δH and Val E11 C_αH peaks,²⁰ respectively. For each metMbcCN complex studied, the ^1H -NMR spectrum exhibits a pair of rapidly relaxing single proton peaks labeled H_j (low field near ~ 15 ppm) and H_z (upfield near -5 to -10 ppm) (Figures 2–10), whose saturation (not shown) provides diagnostic NOE patterns^{17,18} and shifts that unambiguously assign the key amino acid resonances for Phe CD1, C_δH (H_j), $\text{C}_\delta\text{H}_s$ (H_k), and C_βH_s (H_m), and Ile FG5, $\text{C}_\alpha\text{H}'$ (H_w), $\text{C}_\gamma\text{H}_3$ (M_x), C_βH_3 (M_y), and C_γH (H_z), as described in detail elsewhere.^{17,18,20,21} The relative positions of pairs of methyls on the heme is established by the observation of $\sim 5\%$ and $\sim 1\%$ NOEs for methyls on the same pyrrole and methyls adjacent to the same meso position, respectively, as described²¹ in detail for the metMbcCN complex of hemin 2.

The ^1H -NMR spectrum at 25 $^\circ\text{C}$ of metMbcCN reconstituted with hemin 3 is shown in Figure 2B. Saturation of heme methyl peak M_e (Figure 2C) yields NOEs to Phe CD1 $\text{C}_\delta\text{H}_s$ (H_m) and Ile FG5 C_βH_3 (M_y) diagnostic^{17,18,21} of a methyl at position e; saturation of the peak H_f , to which a NOE is detected in Figure 2C, yields a large ($\sim 30\%$) NOE to H_f' (not shown), identifying H_f , H_f' as members of an $\alpha\text{-CH}_2$ adjacent to a heme methyl. These dipolar connectivities, in addition to the clear absence of a methyl signal in the 12–13 ppm due to position h (compare Figure 2A and 2B), dictate the orientation shown in 3 with propionates at positions f, g, and h. The reference trace for metMbcCN reconstituted with hemin 4 is illustrated in Figure 2D. Saturation of M_e (Figure 2E) yields the NOEs to Ile FG5 (M_y) and Phe CD1 (H_m) and a $\sim 1\%$ NOE to M_d , identifying M_e , M_d as methyls at positions e and d, respectively; H_f' is one of a geminal methylene group (the other, H_f , not shown) arising from a propionate $\alpha\text{-CH}_2$ at position f. Irradiation of M_h gives an NOE pattern diagnostic²¹ of position h (not shown), and saturation of M_a (Figure 2F) yields the small NOE to M_h identifying it as the methyl at position a, while the peak H_b , when saturated (Figure 2G), identifies the $\alpha\text{-CH}_2$ peaks H_b , H_b' from the propionates at position b. Hence the orientation is as in 4 with the “odd” propionate at position b.

The equilibrium ^1H -NMR spectrum at 25 $^\circ\text{C}$ of metMbcCN reconstituted with hemin 5 is given in Figure 3A; unlike all other isomers, this complex exhibits two sets of peaks under all conditions, M_i , H_i and m_i , h_i . Similar to Figure 2, the saturation of M_e (Figure 3B) and M_h (Figure 3C) identify methyls at positions e and h, and the $\sim 5\%$ NOEs to M_b and $\sim 1\%$ NOE to M_h upon saturating M_a (Figure 3D) identify methyls uniquely at positions a and b, respectively. Hence the major isomer has the orientation as shown in 5A, with the “odd” propionate at position d. Since saturation of m_h (Figure 3E) and m_b (Figure 3F) fails to give $\sim 5\%$ NOEs to each other or to the third resolved heme methyl, m_e , this isomer cannot have adjacent methyls at either positions a, b or e, f (see Figure 2A) and hence demands the orientation be as in 5B, with the “odd” propionate at position a. The equilibrium ratio of the isomer 5A:5B is $\sim 6:1$ at 25 $^\circ\text{C}$.

The 25 $^\circ\text{C}$ ^1H -NMR traces of metMbcCN complexes of hemins 6 and 7 are shown in Figure 4A, B, respectively; neither exhibits a methyl peak near 12–13 ppm diagnostic for a methyl at position²¹ h, and hence the orientations must be as shown in 6 and 7 in Figure 1, with propionates at the positions g, h and f, h, respectively. These orientations as well as individual assignments are confirmed by saturation of the relevant resonances (not shown). The reference

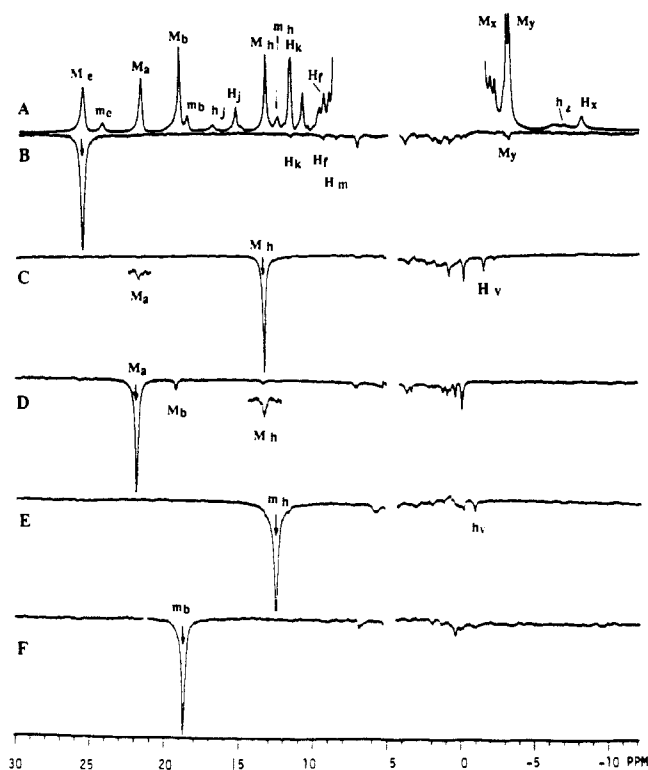


Figure 3. (A) 500-MHz $^1\text{H-NMR}$ reference spectra of hemin 5 in metMbcn in $^2\text{H}_2\text{O}$, pH 7.14 at 25 $^\circ\text{C}$. (B) Saturate major component peak M_e ; note NOEs to Phe CD1 (H_m) and Ile FG5 (M_y) as well as to H_r , the adjacent propionate H_α . (C) Saturate M_h ; note NOEs to M_a and upfield NOEs (indicating Val E11 $C_\alpha\text{H}$, H_v) characteristic of position h. (D) Saturate M_a ; note -5% and -1% NOEs to M_b and M_h , respectively. Saturate minor component peaks m_h (E) and m_b (F); note absence of $\sim 5\%$ NOEs to any other resolved heme methyl resonances, indicating that no two arise from the same pyrrole. The upfield NOEs in (E) are indicative of H_v ($C_\alpha\text{H}$ of Val E11) and hence confirm assignment based on both shift and NOE pattern.

trace for metMbcn reconstituted with hemin 8 is found in Figure 4C. Saturation of M_e (Figure 4D) and M_h (Figure 4E) identifies methyls at positions e and h by the diagnostic NOE pattern to amino acid resonances. The $\sim 5\%$ NOE from M_h to M_g demands a methyl at position g as well and uniquely determines the orientation as in 8 of Figure 1, with propionates at positions b and f.

The reference trace of metMbcn reconstituted with hemin 9 appears in Figure 5A. Irradiation of M_e (Figure 5B) yields characteristic NOEs to H_m and M_y , with $\sim 5\%$ NOEs to M_f identifying methyls at both positions e and f. Saturation of M_h yields NOEs (Figure 5C) diagnostic of a methyl at position h, and the $\sim 1\%$ NOE to M_a identifies the methyl at position a. Saturation of M_a (Figure 5D) yields the reciprocal NOE to M_h and also to H_b , whose irradiation (Figure 5E) locates the geminal partner, H_b' ; both H_b, H_b' arise from the propionate $\alpha\text{-CH}_2$ group at position b. Saturation of M_d locates the adjacent methyl M_c (not shown). The unambiguous orientation is as in 9A, with propionates at positions b and g. The reference $^1\text{H-NMR}$ trace of the metMbcn complex of hemin 10 exhibits five methyls below 10 ppm, which demand methyls in positions a, b, e, f, and h on the basis of Figure 2A. Detailed NOEs upon saturation of M_e , M_f , M_a , and M_h (Figure 6B–E, respectively) assign the methyls M_e , M_a , M_f , M_b , and M_h to the methyls at positions e, a, f, b, and h, respectively, based on the same arguments as presented above for the other complexes. Hence the propionates occupy positions d and g as shown in 10A of Figure 1. The chemical shifts for the metMbcn complexes of the various hemins are listed in Table I.

pH Effects. The optical spectra were found to be essentially pH independent over the range 5.5–10 for the metMbcn complexes studied, as indicated above. The $^1\text{H-NMR}$ spectra for all

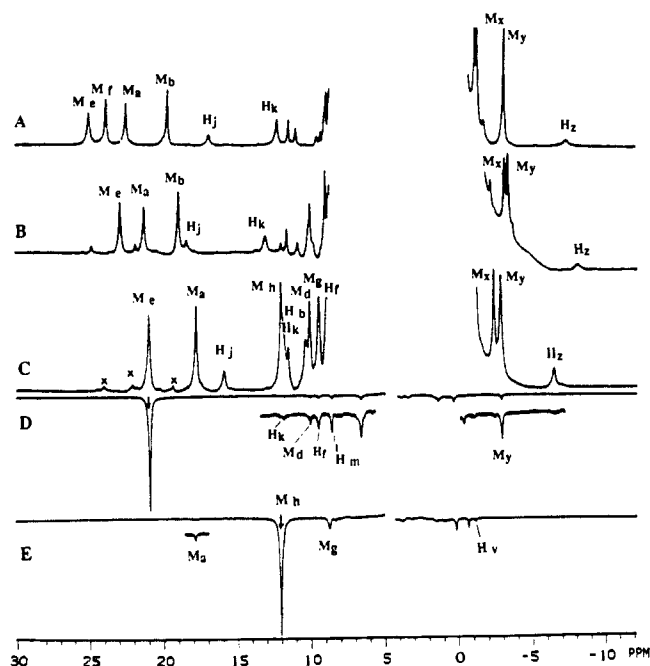


Figure 4. 500-MHz $^1\text{H-NMR}$ reference trace of the metMbcn complex in $^2\text{H}_2\text{O}$ reconstituted with (A) hemin 6, at 25 $^\circ\text{C}$ and pH 8.0, (B) hemin 7, at 25 $^\circ\text{C}$ and pH 8.6, and (C) hemin 8, at 25 $^\circ\text{C}$ and pH 8.6. (D) Saturate M_e for reference trace C above; note characteristic NOEs to Phe CD1 (H_m , H_k) and Ile FG5 (M_y) as well as to M_d and H_r . (E) Saturate M_h ; note characteristic upfield NOEs (including Val E11 $C_\alpha\text{H}$, H_v) and -5% and -1% NOEs to M_g and M_a , respectively.

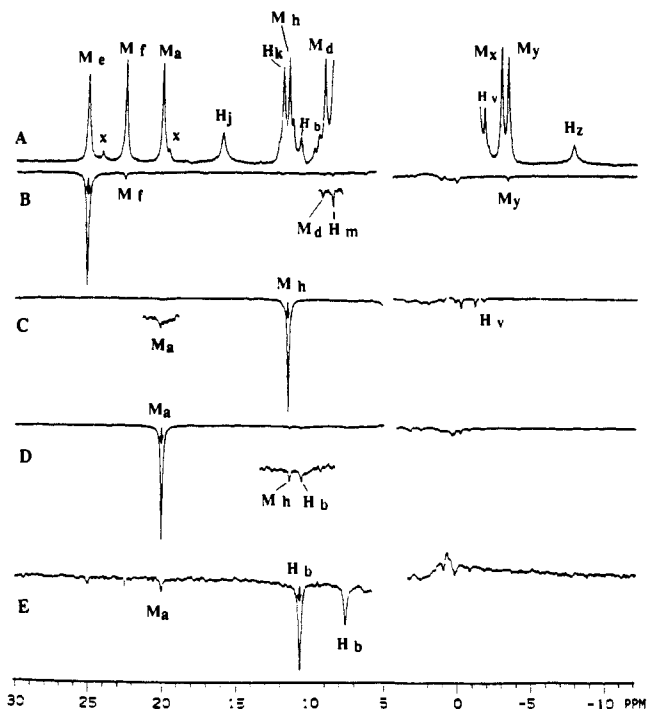


Figure 5. (A) 500-MHz $^1\text{H-NMR}$ reference trace for the metMbcn complex of hemin 9 in $^2\text{H}_2\text{O}$ at pH 8.0 and 30 $^\circ\text{C}$. (B) Saturate M_e ; note $\sim 5\%$ NOE to M_f and characteristic NOEs to Phe CD1 ($C_\beta\text{H}$ (H_m) and Ile FG5 $C_\beta\text{H}_3$ (M_y)). (C) Saturate M_h ; note NOE to M_a as well as characteristic upfield NOEs, including Val E11 $C_\alpha\text{H}$ (H_v). (D) Saturate M_a ; note $\sim 1\%$ NOE to M_h and NOE to H_b . (E) Saturate H_b ; note large NOE to H_b' identifying a geminal $\alpha\text{-CH}_2$ next to M_a .

complexes exhibited weak inflections near pH 5.3 as found for native metMbcn.²⁹ The pH profile for chemical shifts titrating into the strongly alkaline region (to pH 10) were found negligible

(29) Krishnamoorthi, R.; La Mar, G. N. *Eur. J. Biochem.* **1984**, *138*, 135–140.

Table I. Chemical Shifts for metMbCN Complexes Reconstituted with Synthetic Hemin Isomers 3–10^a

	hemin ^b									
	3	4	5	6	7	8	9A	9B	10A	10b
heme ^c										
a ^e	23.1	19.9	21.8	23.0	21.3	18.7	20.4	18.7	22.7	20.4
b ^e	19.8	[10.8]	19.2	19.1	19.0	[11.1]	[10.9]	17.1	19.8	18.2
c ^e	5.7	5.7	6.0	5.7	5.6	5.6	5.7	10.8	6.0	<i>d</i>
d ^e	8.8	9.9	<i>d</i>	8.7	10.0	10.3	9.0	10.8	<i>d</i>	13.5
e ^e	25.0	24.4	25.7	25.4	23.0	22.2	25.5	<i>d</i>	26.5	24.9
f ^e	[10.7]	[9.3]	[9.4]	24.1	[9.0]	[9.5]	22.8	19.5	21.3	23.0
g ^e	<i>d</i>	<i>d</i>	<i>d</i>	<i>d</i>	<i>e</i>	8.8	<i>d</i>	10.3	<i>d</i>	<i>e</i>
h ^e	<i>d</i>	12.32	13.3	<i>d</i>	<i>d</i>	12.3	11.6	<i>d</i>	12.7	<i>d</i>
Phe CD1 C ₇ H(H _z)	17.3	16.4	15.4	17.2	18.4	16.9	16.2	<i>f</i>	14.0	<i>f</i>
Phe CD1 C ₈ Hs(H _k)	12.5	11.9	11.6	12.4	11.6	12.0	12.0	<i>f</i>	11.4	<i>f</i>
Phe CD1 C ₈ Hs(H _m)	9.0	9.0	8.5	8.6	8.6	8.5	8.6	<i>f</i>	8.4	<i>f</i>
Val E11 C _α H(H _e)	-2.0	-2.2	-2.3	-1.4	-2.3	-1.8	-1.9	-0.3	-1.4	<i>f</i>
Ile FG5 C _γ H'(H _w)	-1.8	-1.7	-2.0	-1.2	-1.4	-1.1	-1.3	-0.8	-1.9	<i>f</i>
Ile FG5 C _γ H ₃ (M _z)	-3.4	-3.1	-3.1	-3.3	-3.2	-2.8	-3.0	-1.8	-2.9	<i>f</i>
Ile FG5 C _δ H ₃ (M _y)	-3.6	-3.7	-3.3	-3.3	-3.4	-3.3	-3.5	-2.5	-2.9	<i>f</i>
Ile FG5 C _γ H(H _z)	-8.7	-8.6	-8.2	-7.7	-8.1	-7.4	-8.1	-5.6	-7.6	<i>f</i>

^aShifts in ppm from DSS in ²H₂O solution at 25 °C, pH 8. ^bStructure and orientation of heme as defined in Figure 1. ^cMethyls and, in brackets, propionate H_αs. ^dPropionate H_α peaks expected under diamagnetic envelope are not assigned. ^eHeme methyl peaks expected to resonate under diamagnetic envelope are not assigned. ^fNot assigned. ^gPeak.

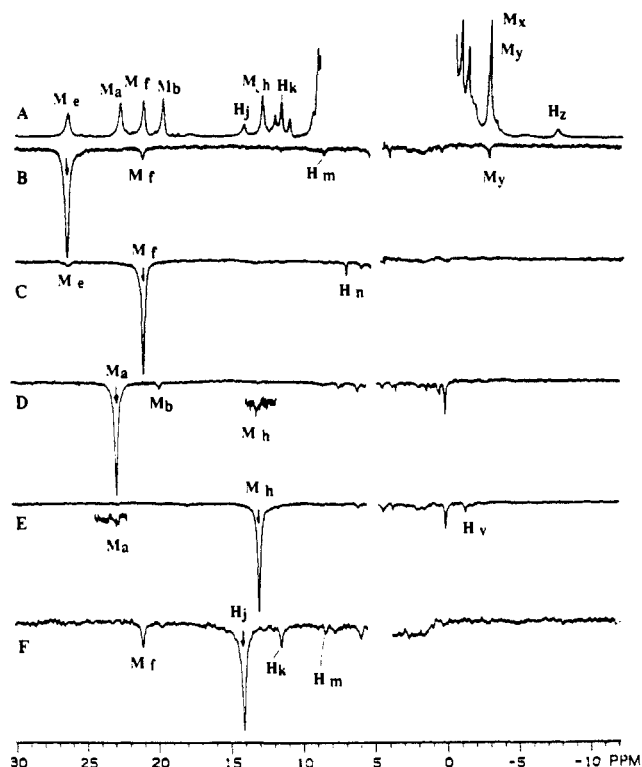


Figure 6. (A) 500-MHz ¹H-NMR reference trace for the metMbCN complex of hemin 10 in ²H₂O at pH 6.4 at 25 °C. (B) Saturate M_e; note ~-5% NOE to M_f and characteristic NOEs to Phe CD1 C₈Hs (H_m) and Ile FG5 C_γH₃ (M_y). (C) Saturate M_f; note reciprocal NOE to M_e and NOE to sharp peak at 7 ppm due to His FG3 C_βH (H_n). (D) Saturate M_a; note ~-1% NOE to M_h. (E) Saturate M_h; note reciprocal small NOE to M_a as well as upfield NOE characteristic for position h. (F) Saturate Phe CD1 C₇H peak H_j; note NOEs to other Phe CD1 peaks H_k and H_m but also to M_f rather than M_e.

for the peaks of the species that exist at acidic to neutral pH. In the metMbCN complexes of hemins 2, 4, 5, and 6, the species characterized at neutral pH remained intact to pH 10 without any inflection in the chemical shift profiles or changes in peak intensities (not shown).

For the metMbCN complexes of both hemins 9 and 10, the neutral pH resonances, M_i, H_i, lose intensity upon raising the pH, simultaneously giving rise to a new set of resonances, M_i^{*}, H_i^{*}, with relative ratios ~3:1 indicative of methyls and single protons (Figures 7 and 8, respectively). The shift values for the new complexes are included in Table I. In the complex of hemin 9,

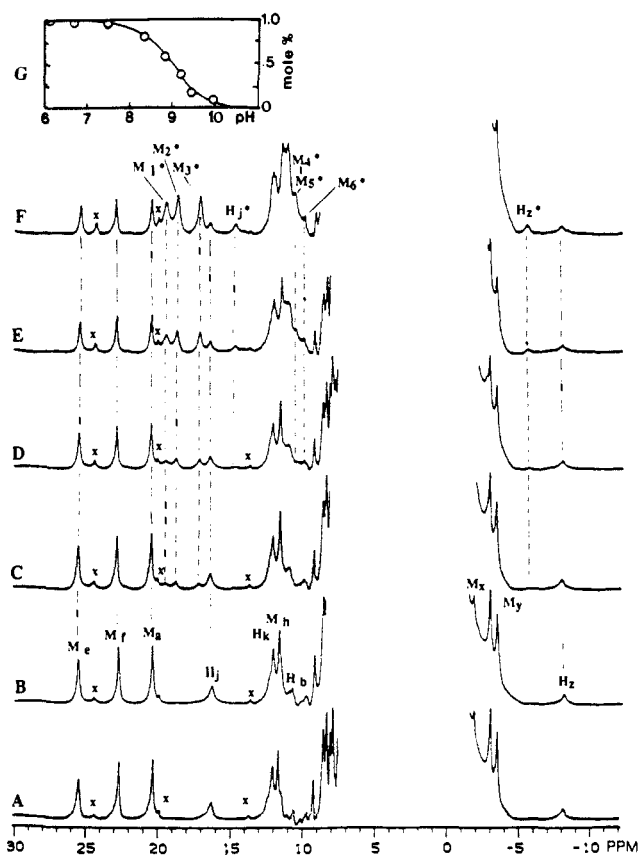


Figure 7. 500-MHz ¹H-NMR trace of the metMbCN complex of hemin 9 in ²H₂O at 25 °C as a function of pH (A) 6.64, (B) 7.50, (C) 8.38, (D) 8.82, (E) 9.19, and (F) 9.46. The peaks are labeled as in the caption for Figure 2; × indicates peaks of hemin impurity also observed in free hemin. Note the gradual loss of intensity without shift changes for peak M_i, H_i as the pH is raised into the alkaline region, concomitant with the appearance of a new set of peaks M_i^{*}, H_i^{*} with pH-independent shifts. A plot of mole fraction neutral pH isomer as a function of pH is shown in (G) and yields an apparent pK ~9.0.

resolved methyl peaks M₁^{*}, M₂^{*}, and M₃^{*} and single proton H_z^{*} replace M_e, M_f, M_a, M_h, and H_z (Figure 7). Integration of peaks M_e and M₃^{*} as a function of pH (or H_z and M₂^{*}) indicates an apparent pK ~9.0 (Figure 7G). The pH profile of the metMbCN complex of hemin 10 exhibits similarly pH independent shifts for the peaks M_e, M_a, M_f, M_b, and M_h (Figure 8A), which lose their intensity as they broaden slightly (pH 7–8) and are replaced by a new set of pH-independent resonances, M₁^{*}, M₂^{*}, M₃^{*}, M₄^{*},

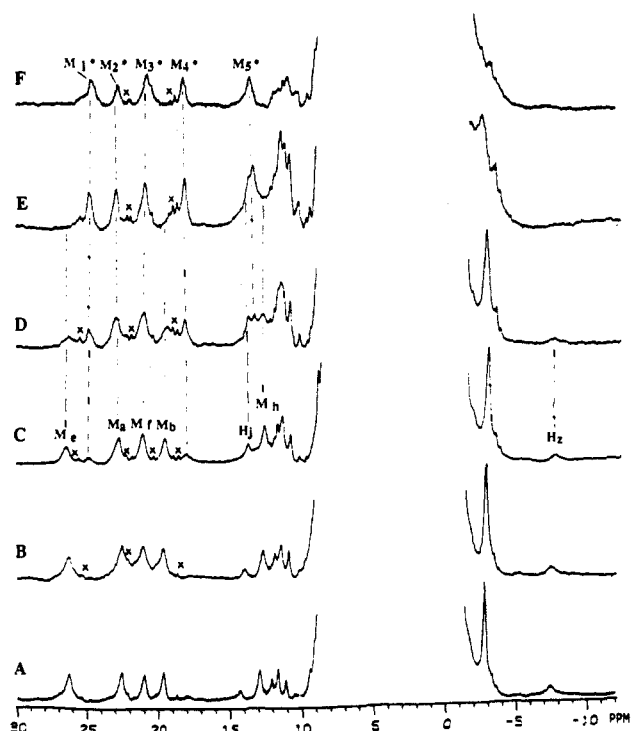


Figure 8. 500-MHz ¹H-NMR trace of the metMbcCN complex of hemin 10 in ²H₂O at 25 °C as a function of pH: (A) 6.60, (B) 7.18, (C) 7.63, (D) 8.04, (E) 8.57, and (F) 9.15. Small sharp impurity peaks are designated x. Note the general loss of intensity of the M₁, H₁ peaks with pH-independent shifts as the pH is raised, with the parallel appearance of a new set of peaks M₁^{*}, H₁^{*} whose shifts are also pH independent.

and M₅^{*} (Figure 8F). For this complex, integration reveals that peaks M_a, M₂^{*} and M_f, M₃^{*} are nearly degenerate. Estimation of the relative intensities of methyl peaks M_e, M₄^{*} yields an apparent pK in the range 8.0–8.2. The metMbcCN complex of hemin 5 also exhibited complex changes with pH above pH 8 that indicated multiple sets of resonances, some broadened extensively, indicative of more than one species. It was not possible to connect the resonances to individual species (see supplementary material). Since the protein tended to precipitate above pH 8.5, further characterization was not pursued.

Saturation-Transfer Determination of Heme Orientation at Alkaline pH. The identity of the alkaline molecular species giving rise to the sets of resonances M_i^{*}, H_i^{*} for the metMbcCN complex of hemins 9 and 10 can be established solely on the basis of the hyperfine shift pattern^{21–23} if the assignments of the heme resonances can be effected. Figure 9A illustrates the ¹H-NMR trace of the metMbcCN complex of hemin 9 at 25 °C which exhibits an M_i:M_i^{*} intensity ratio of ~2:1. Saturation of resolved alkaline isomer peaks M₁^{*} (Figure 9B), M₂^{*} (Figure 9C), and M₃^{*} (Figure 9D) each leads to a difference trace intensity only for the assigned neutral pH isomer peaks, M_h, M_c, and M_d, respectively. Since the peaks M_i and M_i^{*} belong to different species at equilibrium, the saturation transfer between the two species must arise from the magnetization transfer that accompanies chemical exchange in the regime where the exchange rate, *k*, is of the same order as the inverse intrinsic relaxation time of the detected peak.³⁰ It is noted that none of the low field methyls M₁^{*}–M₃^{*} NOEs in the upfield region (Figure 9A–C) where Ile FG5 C_γH₃ is observed when the upfield C_γH peak (H_z^{*}) is saturated (not shown), indicating that M₁^{*}, M₂^{*}, and M₃^{*} do not occupy the e position in the heme pocket. Conversely, saturation of the low field neutral pH isomer peaks at 30 °C (reference trace in Figure 9E), M_e (Figure 9F) and M_a (Figure 9G), yields, in addition to the NOEs to resonances of the same isomer defined in Figure 5, intensity in the difference trace for peaks M₄^{*} and M₆^{*}, respectively.

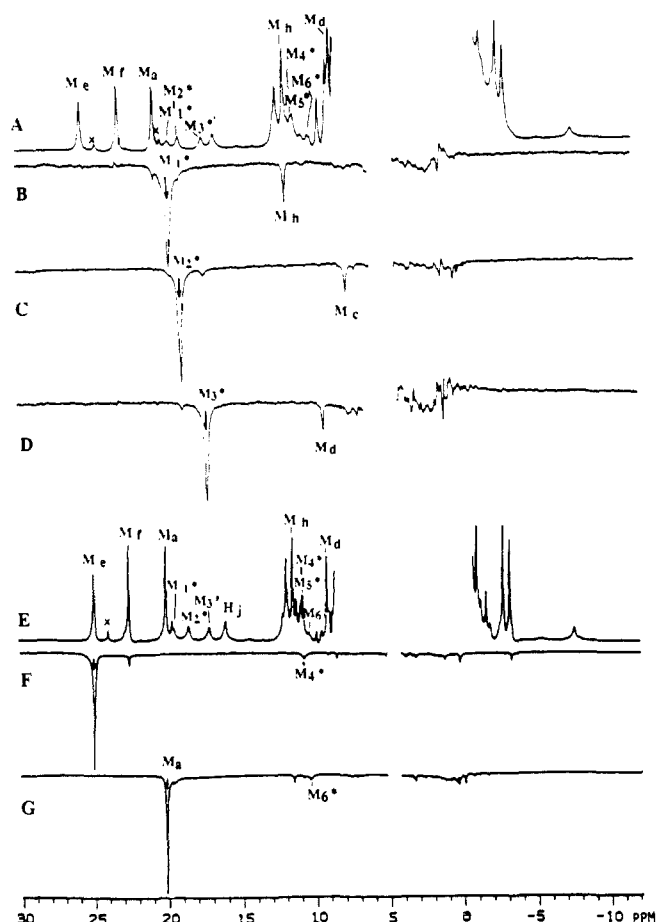


Figure 9. 500-MHz ¹H-NMR reference spectrum of the metMbcCN complex of hemin 9 in ²H₂O, pH 8.8, where the position of the equilibrium 9A ⇌ 9B yields a ratio of M_i:M_i^{*} of ~2.1 (A) at 25 °C and (E) at 40 °C. The peak labels for the two species are the same as in Figure 5. Saturation of alkaline pH isomer peaks M₁^{*} (B), M₂^{*} (C), and M₃^{*} (D) results in saturation transfer to the assigned neutral pH isomer peaks, M_h, M_c, and M_d, respectively. Saturation of the neutral pH form peaks M_e (F) and M_a (G) gives rise, in addition to intramolecular NOEs described in Figure 6, to saturation transfer to alkaline isomer peaks M₄^{*} and M₆^{*}, respectively.

Saturation of M_f similarly connects to M₅^{*}, just to the low field side M₄^{*} (not shown). Comparison with the expected contact shift pattern in Figure 2A dictates that the interconversion of the methyl peaks M_i with large contact shifts for the neutral pH isomer with methyls M_i^{*} with small contact shifts for the alkaline isomer can only occur if the two heme orientations differ by a 90° rotation about the heme normal or a 180° rotation about a meso-iron-meso axis bisecting positions b and c (and f and g). However, the latter possibility (which would place propionates to positions c and f) would place a methyl at position e, which is contradictory to the absence of an NOE from any of the low field methyls to Ile FG5 peaks. Hence the alkaline isomer must have the structure as in 9B of Figure 1.

The reference trace of the metMbcCN complex of hemin 10 at 25 °C and pH 7.6 is shown in Figure 10A with the position of the peaks for the identified neutral pH isomer, 10A, labeled M_i and the positions of the alkaline isomer methyl peaks designated M₁^{*}–M₆^{*}, as indicated in Figure 6. Saturation of M_e leads to saturation transfer³⁰ to resolved peak M₂^{*} (Figure 10B). Irradiation of the composite M_a, M₂^{*} leads to the expected reciprocal saturation transfer from M₂^{*} to M_e, but the appearance of M₄^{*} in the difference trace must arise from saturation transfer from M_a (Figure 10C). Saturation of M_b (Figure 10D) leads to saturation transfer to M₃^{*} under M_f (M_b and M_f are not diplac coupled; see Figure 5D), while saturation of M_h leads to saturation transfer to M₆^{*} (Figure 10E). The complete interconvertibility of the two sets of resonances is depicted schematically in Figure 10F. It is noted that the pattern of the contact shifted methyl

(30) Sandström, J. *Dynamic NMR Spectroscopy*; Academic Press: New York, 1981; Chapter 5.

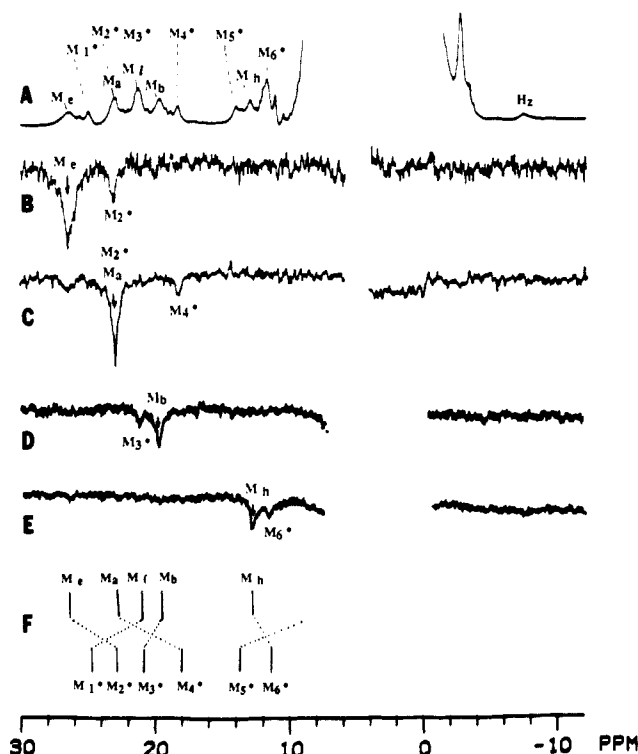


Figure 10. 500-MHz $^1\text{H-NMR}$ reference spectrum of the metMbcCN complex of hemin **10** in $^2\text{H}_2\text{O}$, pH 7.7, at 25°C , where the equilibrium **10A** \rightleftharpoons **10B** yields a ratio $M_1:M_1^*$ of $\sim 3:1$. The peak labels for the two species are the same as in Figure 6. (B) Saturation of the neutral pH isomer peak M_2 leads to a $\sim 40\%$ saturation transfer to M_2^* . (C) Saturating the composite M_2, M_2^* yields the reciprocal effect from M_2^* to M_2 and saturation transfer from M_2 to M_4^* . Similarly, saturation of resolved peak M_b (D) and M_h (E) yield saturation transfer to M_3^* and M_6^* , respectively. The saturation-transfer connectivities for the set M_i to M_i^* are illustrated schematically in (F).

resonances in the two isomers is essentially the same, with five resonances downfield of 10 ppm in each isomer. The expected contact shift pattern for methyls in the eight possible environments as depicted in Figure 2A demand, therefore, that *both isomers* have methyls at positions a, b, e, f, and h. Since the NOE-determined orientation for the neutral pH isomer is that depicted in **10A** of Figure 1, the alkaline pH isomer must be that depicted in **10B**, with the interconversion between the two involving a 180° hopping about the iron–His bond. Comparison of the two orientations indicate that, while the environments are interchanged between the pairs of pyrroles with either large (pairs a, b and e, f) or small (c, d and g, h) contact shifts, the relative position of site a versus b and e versus f are interchanged, which is completely consistent with the pattern of two low field methyls (or two high field) exchanging positions as shown in Figure 10F.

Discussion

Comparison of Spectral Properties. Each of the synthetic hemins **2–10** incorporate cleanly into the heme pocket of sperm whale Mb at acidic to neutral pH, in spite of the fact that several of the hemes demand that propionates occupy highly hydrophobic sites in the interior of the protein. In fact, each of the eight positions are occupied by a propionate group for at least one of the hemins. The largely retained structural integrity of the heme pocket is witnessed not only in the conserved optical spectra but also in the NMR spectral characteristic of both the metquo and metcyano complexes. The large hyperfine shifts in the paramagnetic derivatives provide particularly sensitive probes of molecular/electronic structural perturbations.^{24,31} The metMbH₂O samples of hemins **3–10** all exhibit hyperfine shift patterns very similar to those of the native protein.^{25,32} In particular, the narrow 20-ppm peak indicative of the propionate orientation at the g position (7-propionate of native hemin), which makes a salt bridge to His FG3, is observed for all hemins except **7** and **8**, arguing

against a propionate at this position (see supplementary material). The determination of the orientations in the metMbCN complexes quantitatively bears out this conclusion and affirms the essential feature of the native pocket for all of the hemins.

In the metMbCN complexes, Phe CD1 and Ile FG5 dipolar shifts of very similar magnitude (Table I) argue for retained orientation of those residues as well as conservation of the magnetic properties of the iron,^{24,31,33} except for select hemins considered below (hemins **5** and **9**). The adherence of the methyl contact shift patterns for all hemins (except hemin **9** at alkaline pH, i.e., **9B**) to that described for native protohemin as well as a large variety of hemins²¹ with solely the "normal" propionate at positions f and g (i.e., Figure 2A) provides additional support for the largely invariant seating of the heme skeleton in the pocket (i.e., **1** in Figure 1), with essentially the same disposition relative to a fixed His F8 imidazole orientation.^{23,24}

The ability of the folded Mb holoprotein to accommodate such a diversity of perturbed hemins without apparent loss of the pocket structure is evidence for the remarkable resilience or adaptability of the heme pocket, both from the point of steric accommodation for the large propionate groups as well as bringing polar side chains into apparently hydrophobic regions. The steric accommodation of the pocket in Mb had been observed for similarly large, although nonpolar peripheral substituents in place of vinyls of protohemin.¹² The behavior of the Mb pocket with respect to hydrophilic side chains is in sharp contrast to that of cytochrome *b₅*, where the ability of the heme pocket to accommodate non-native propionate groups without losing the prosthetic group binding ability is severely limited.³⁴

Propionate pKs. Prior to evaluation of the relative preferences for propionate side chains occupying non-native heme pocket sites, the states of protonation must be ascertained. An exposed heme propionate, in common with alkyl carboxylic acids, exhibits $pK \sim 4\text{--}5$, and the pK s of the native 6,7-propionates at positions f and g have been assumed near normal.^{29,35} The observed native metMbCN $pK \sim 5.3$ has been associated²⁹ with the 7-propionate (position g), and the 6-propionate (position f) must have a similar or lower pK since it extends toward the protein exterior; the absence of $pKs > 5.3$ in the NMR spectra of metMbCN supports this view.²⁹ The pH profiles of the metMbCN complexes of hemins **3**, **4**, **6** and **7** are essentially the same as for native metMbCN²⁹ to pH 10, exhibiting only the inflection indicative of $pK \sim 5.3$ (not shown) for these hemins. Hence the odd propionate pK s are either < 5.2 or > 10 . For the odd propionate at position h (i.e., hemins **3**, **6**, and **7**), the structure as revealed through molecular graphics suggests that the propionate may be extended toward the pocket to which water has access. Hence we suggest that the propionate at position h is ≤ 5.2 and therefore is deprotonated in the pH range 6–10. Conversely, the propionate at position b (i.e., hemins **4**, **8**, and **9** at neutral pH, i.e., **9A**) is in a highly hydrophobic region² and could not have a $pK \leq 5.2$. This is confirmed by the dramatic structural conversion for **9A** \rightleftharpoons **9B** with apparent pK 9.0. Since the pK for the g position propionate is 5.3,²⁹ the $pK \sim 9.0$ (Figure 7) *must represent the deprotonation of the b position propionate*. For hemin **9**, the deprotonation results in a more stable orientation with the two ionized carboxylates at positions e and h (**9B**) rather than b and g (**9A**). Conversely, since hemins **4** and **8** cannot find alternate orientations, their apparent pK s for the b propionate groups must be > 10 .

Similarly, since the f, g propionate pK s are ≤ 5.3 , structural conversion **10A** \rightleftharpoons **10B** centered at pH ~ 8.1 (Figure 6) must represent the pK of the propionate at position d. The metMbCN complex of hemin **5** exhibits a similar perturbation at pH ~ 8 but does not lead to a single identifiable product at higher pH. The

(31) Satterlee, J. D. *Annu. Rept. NMR Spectrosc.* **1985**, *17*, 79–178.

(32) Unger, S. W.; Lecomte, J. T. J.; La Mar, G. N. *J. Magn. Reson.* **1985**, *64*, 521–526.

(33) Emerson, S. D.; La Mar, G. N. *Biochemistry* **1990**, *29*, 1556–1566.

(34) Lee, K.-B.; La Mar, G. N.; Pandey, R. K.; Rezzano, I. N.; Mansfield, K. E.; Smith, K. M.; Pochapsky, T. C.; Sligar, S. G. Submitted for publication.

fact that the minor component peaks, m_i , for hemin **5B** disappear in the same pH region (see supplementary material) as for peaks M_i , we conclude that the a position propionate also has an apparent $pK \geq 8$.

Thus, although the polar propionic acid side chains can occupy positions in the hydrophobic region of the heme cavity, they exist in the protonated, un-ionized form. The carboxylic acid pK_s of each of the positions a, b, and d are extraordinarily elevated³⁵ values by 3 to 4 pH units and represent destabilization of the charged form by ~ 4 to 4.5 Kcal/mol relative to an exposed carboxylate, confirming the strong hydrophobicity of this position of the pocket. Similarly elevated amino acid carboxylate pK_s have been observed in proteins when concealed in a hydrophobic crevice.³⁵ This destabilization must result in a comparable decrease in the heme binding free energy for the complex. The fact that Mb can absorb this destabilization and still maintain tight heme binding is witness to the extraordinary stability of the heme-protein interaction. Conversely, it may be expected that the forced accommodation of two propionates at interior hydrophobic sites could sufficiently destabilize the heme binding so as to preclude holo-protein formation. Preliminary data indicate that this is the case.³⁶

Propionate Orientational Preferences. The hemins **3**, **4**, and **5** were designed to provide the standard salt bridges at both positions f and g, with the odd propionate providing direct preferences for the pairs at positions e versus h (hemin **3**), b versus c (hemin **4**) and a versus b (hemin **5**). Estimating that a 3% minor orientation could have been detected for hemins **2** and **3**, the positions b and h are more stable than c and e, respectively, by ≥ 2 Kcal, while the 6:1 ratio of **5A**:**5B** indicates the d position is more stable than the a position by ~ 1.5 Kcal. We note that neither the c nor e position is detectably populated by a neutral propionate in any of the complexes, but both are occupied by the ionized side chain in **9B** and **10B**, but only when both propionates are at non-native orientations.

The strong preferences of positions d and b over a and c are likely not determined primarily by differential hydrophobic effects but by steric constraints, since the native Mb pocket exhibits^{1-3,7,8,12} a strong preference (>2 Kcal/mol) for the vinyls at positions b and d over a and c. For the b position, the accommodation of the propionates with $pK > 10$ represents extraordinary stability with negligible perturbation of NMR spectral indicators of heme pocket structure, which may be explained by the intercalation of the propionate side chain into the hydrophobic cavity or "xenon hole" on the proximal side of the heme.^{2a} In the d position, there is no preformed cavity for such a large side chain as a propionate. Possible structural accommodations to seat a propionate at position d are indicated both by differences in amino acid dipolar shift patterns and select NOE connectivities for complexes hemins **5** and **10**. Both exhibit normal Ile FG5 shifts, as found for the other complexes and native metMbCN^{17,24} (Table I); even the NOE pattern between the heme methyls and Ile FG5 for hemins **5** and **10** are essentially the same as those for the other complexes (Figures 3 and 8). On the other hand, the Phe CDI shifts

(particularly for hemin **5**) are both smaller than for other complexes^{18,20,21} (see Figures 3 and 6 and Table I), and the NOE pattern between the heme and Phe CDI is perturbed. Thus for **10A**, the NOE to Phe CDI C_β Hs from M_f and not M_e (C_β Hs or C_γ H also give NOEs to M_f rather than M_e ; not shown). The altered shifts and NOE patterns are consistent with the movement of the Phe CDI side chain away from the position over the meso position between positions d and e and toward position f, the likely result of trying to accommodate the propionate side chain. Since the perturbation to shifts and NOEs is select to Phe CDI and leaves Ile FG5 largely unaffected, we conclude that the d position propionate is oriented toward the distal side of the heme.

The most perturbed NMR spectrum observed for the hemins **2-10** is that for the alkaline form or deprotonated form of **9** (i.e. **9B** in Figure 1), as shown in Figure 7F. The methyl shift spread, while indicative of the same rhombic perturbation, is considerably reduced in asymmetry, with all six methyls resonating between 10 and 20 ppm.^{21,23,24} This could result from a slight rotation of the hemin counterclockwise about the His-iron bond, in **9B** of Figure 1, so that the His F8 more closely bisects the meso-Fe-meso than N-Fe-N axis. Such an orientation is predicted to result in a decrease in the shift spread²³ and has been observed in *Aplysia* Mb⁹ where the His F8 is rotated similarly in the ground-state structure.³⁷ This unique proposed perturbation of the heme cavity structure could result from trying to avoid the very unfavorable contact between the structurally highly conserved Phe CDI and the ionized propionate at position e.

Heme Pocket Dynamics. The nonselective T_1 s of heme methyls in a variety of metMbCN complexes of modified hemins have been shown to be in the 100-150 ms range.^{17,18,20,21} Hence the ~ 10 -40% saturation transfers observed in the **9A** \rightleftharpoons **9B** and **10A** \rightleftharpoons **10B** interconversions represent lifetimes in the 0.1-1-s range.³⁰ These interconversions can occur simply by rotational hopping about an intact His-iron bond and have lifetimes comparable to those reported for the rotational hopping of 4-fold symmetric synthetic hemins without propionates.^{38,39} The similar lifetimes observed here for hemins with propionates argue against conclusions that this rapid rotational hopping for the nonpolar hemins was possible solely because of the absence of propionate side chains.³⁹ Preliminary results indicate that the variations of both propionate pK_s and the dynamics of interconversion of alternate forms can serve as sensitive probes of heme pocket structural differences in genetic variants of Mb.

Acknowledgment. This research was supported by grants from the National Institutes of Health, HL-16087 and HL-22252.

Supplementary Material Available: 360-MHz ¹H-NMR spectra of MetMbH₂O complexes of hemins **2-10**, a table of the shifts for the resolved resonances, and a figure showing the effect of pH on the 500-MHz ¹H-NMR spectrum of the metMbCN complex of hemin **5** (3 pages). Ordering information is given on any current masthead page.

(35) Parsons, S. M.; Raftery, M. A. *Biochemistry* **1972**, *11*, 1633-1638.

(36) La Mar, G. N.; Hauksson, J. B.; Dugad, L. B.; Venkataramana, N.; Smith, K. M. Unpublished observations.

(37) Bolognesi, M.; Onesti, S.; Gatti, G.; Coda, A. *J. Mol. Biol.* **1989**, *205*, 529-544.

(38) Neya, S.; Funasaki, N. *J. Biol. Chem.* **1987**, *262*, 6725-6768.

(39) Neya, S.; Funasaki, N. *Biochim. Biophys. Acta* **1988**, *952*, 150-157.